AD-A233 251

THE JOURNAL OF BIOLOGICAL CHEMISTRY

DTIC FILE COPY

Vol. 265, No. 24, Issue of August 25, pp. 14127-14135, 1990
Printed in U.S.A.

Structure of a Streptococcal Adhesin Carbohydrate Receptor*

(Received for publication, February 13, 1990)

Frederick J. Cassels‡§, Henry M. Fales¶, and Jack London‡

From the ‡National Institute of Dental Research and the ¶National Heart, Lung and Blood Institute, National Institutes of Health, Bethesda, Maryland 20892

Russell W. Carlson and Herman van Halbeek

From the Complex Carbohydrate Research Center and Department of Biochemistry, The University of Georgia, Athens, Georgia 30602

Interactions between complementary protein and carbohydrate structures on different genera of human oral bacteria have been implicated in the formation of dental plaque. The carbohydrate receptor on *Streptococcus sanguis* H1 (one of the primary colonizing species) that is specific for the adhesin on *Capnocytophaga ochracea* ATCC 33596 (a secondary colonizer) has been isolated from the streptococcal cell wall, purified, and structurally characterized. The hexasaccharide repeating unit of the polysaccharide was purified by reverse-phase, amino-bonded silica, and gel permeation high performance liquid chromatography. Earlier studies established that the repeating unit was a hexasaccharide composed of rhamnose, galactose, and glucose in the ratio of 2:3:1, respectively. In the present study, determination of absolute configuration by gas chromatography of the trimethylsilyl (+)-2-butyl glycosides revealed that the rhamnose residues were of the L configuration while the hexoses were all D. ^{252}Californium plasma desorption mass spectrometry of the native, the acetylated and the reduced and acetylated hexasaccharide determined that the molecular mass of the native hexasaccharide was 959, and that the 2 rhamnose residues were linked to each other at the nonreducing terminus of the linear molecule. Methylation analysis revealed the positions of the glycosidic linkages in the hexasaccharide and showed that a galactose residue was present at the reducing end. The structural characterization of the hexasaccharide was completed by one and two dimensional ^{1}H and ^{13}C NMR spectroscopy. Complete ^{1}H and ^{13}C assignments for each glycosyl residue were established by two-dimensional (^{1}H,^{1}H) correlation spectroscopy, homonuclear Hartmann-Hahn, and (^{13}C,^{1}H) correlation experiments. The configurations of the glycosidic linkages were inferred from the chemical shifts and coupling constants of the anomeric ^{1}H and ^{13}C resonances. The sequence of the glycosyl residues was determined by a heteronuclear multiple bond correlation experiment. These data show that the structure of the hexasaccharide repeating unit derived from the cell wall polysaccharide of *S. sanguis* H1 is: α-L-Rha*p*-(1→2)-α-L-Rha*p*-(1→5)-α-D-Gal*p*-(1→3)-β-D-Gal*p*-(1→4)-β-D-Glc*p*-(1→3)-α/β-D-Gal.

Protein-carbohydrate interactions appear to be necessary for initial attachment essential in the infection process of viruses (1, 2), mycoplasma (3, 4), protozoa (5-7), and bacteria (8-10). Receptors for microbial carbohydrate-binding proteins have been found on glycolipids (10, 11), glycoproteins (12-14), and on bacterial polysaccharides (15-17). With a more complete understanding of the molecular mediators involved in attachment, therapeutics may be designed to effectively interrupt the process and obviate the attachment altogether (18, 1).

In the human oral environment, a tremendous diversity of microbes interact in a complex ecosystem. This diversity is manifested in dental plaque, consisting of numerous microbes, salivary components, and extracellular bacterial polymers. Intergeneric coaggregation (specific bacterial interactions dependent on adhesin to carbohydrate binding) appears to play a role in the establishment and maturation of dental plaque (19, 20). Coaggregation may occur between genetically unrelated Gram-positive, Gram-negative, or between Gram-negative and Gram-positive partners. Many of these coaggregations are inhibitable *in vitro* by simple sugars such as lactose, L-rhamnose (Rha),[1] *N*-acetylgalactosamine (GalNAc), and *N*-acetylneuraminic acid. Of the bacteria found in dental plaque, *Streptococcus sanguis*, *Actinomyces viscosis*, and *Actinomyces naeslundii* are the predominant primary colonizers and each is prevalent in mature dental plaque.

Three bacterial polysaccharides that appear to act as adhesin receptors have been studied in detail to date. *S. sanguis* strain H1 coaggregates with *Capnocytophaga ochracea* ATCC 33596 (16), while both *S. sanguis* strain 34 and *S. sanguis*

* This investigation was supported in part by the Department of Energy (DOE) Grant DE-FG09-87ER13810, as part of the United States Department of Agriculture/DOE/National Science Foundation Plant Science Centers program and in part by the Warner-Lambert Company. A preliminary account of this investigation was presented at the 18th Meeting of the Society for Complex Carbohydrates, Ann Arbor, MI, November 8-11, 1989. For the abstract of this presentation, see Van Halbeek, H., Carlson, R. W., London, J., and Cassels, F. (1989) *Glycoconjugate J.* **6**, 422. The costs of publication of this article were defrayed in part by the payment of page charges. This article must therefore be hereby marked "*advertisement*" in accordance with 18 U.S.C. Section 1734 solely to indicate this fact.

§ To whom correspondence should be addressed: Dept. of Gastroenterology, Bldg. 40, Rm. 2088, Walter Reed Army Institute of Research, Washington, DC 20307. Tel.: 202-576-2582.

[1] The abbreviations used are: Rha, L-rhamnose; HPLC, high performance liquid chromatography; HPTLC, high performance thin-layer chromatography; GC/MSD, gas chromatography with mass-selective detection; GLC, gas-liquid chromatography; PDMS, ^{252}Cf-plasma desorption mass spectrometry; COSY, two-dimensional (^{1}H,^{1}H) shift correlation spectroscopy; f.i.d., free-induction decays; HOHAHA, homonuclear Hartmann-Hahn spectroscopy; TPPI, time-proportional phase incrementing; HETCOR, two-dimensional (^{13}C,^{1}H) shift correlation spectroscopy; HMQC, heteronuclear multiple quantum coherence spectroscopy; HMBC, heteronuclear multiple bond correlation spectroscopy; PMAA, partially methylated alditol acetates; FAB, fast atom bombardment.

This document has been approved for public release and sale; its distribution is unlimited.

91 3 07 010

strain J22 are responsible for the coaggregation with *A. viscosis* T14V (15, 17). The former mediates an interaction between Gram-positive and Gram-negative cell types, while the latter two are responsible for the interaction between two Gram-positive partners. The *S. sanguis* 34 coaggregation carbohydrate receptor moiety is a cell wall polysaccharide consisting of hexasaccharide repeating units with intrachain phosphodiester linkages (15, 21). The *S. sanguis* J22 receptor is a cell wall polysaccharide composed of a heptasaccharide subunit linked by phosphodiester bonds (17). The coaggregation polysaccharide from *S. sanguis* H1 is also a cell wall polysaccharide, consisting of monophosphorylated hexasaccharide repeating units (16). The glycosyl residues that constitute each respective repeating unit vary, with Rha, Gal, Glc, and GalNAc present in a ratio of 1:2:1:2 in *S. sanguis* 34, Rha, Gal, Glc, and GalNAc (2:2:1:2) in *S. sanguis* J22, and Rha, Gal, and Glc (2:3:1) in *S. sanguis* H1. The present study describes the structural characterization of the hexasaccharide repeating unit from the coaggregation polysaccharide of *S. sanguis* H1.

EXPERIMENTAL PROCEDURES

Bacterial Culture Conditions—*S. sanguis* H1 and *C. ochracea* ATCC 33596 were obtained from Dr. P. Kolenbrander (National Institute of Dental Research). All cells were grown under anaerobic conditions. *S. sanguis* H1 was grown in a complex medium containing Tryptone, yeast extract, Tween 80, and K_2HPO_4 with 0.3% glucose (22), and *C. ochracea* ATCC 33596 was cultivated in Schaedler broth (BBL, Microbiology Systems).

Hexasaccharide Purification—A modification of an earlier procedure (16) giving increased yield of purified hexasaccharide was utilized. Briefly, intact *S. sanguis* H1 cells were sequentially treated with 0.1% Triton X-100, 0.1% Pronase (Calbiochem), and 6 M guanidine HCl, with extensive washing after each treatment. This crude cell wall preparation was then digested by incubation with 26 mg/ml (corresponding to 4 mg/g initial wet weight *S. sanguis* H1 cells) mutanolysin (Sigma). The mutanolysin extract was clarified by centrifugation and the supernatant adjusted to a concentration of 5% trichloroacetic acid. After centrifugation, the supernatant was neutralized, dialyzed extensively against water and lyophilized. Lyophilized material was treated with 48% hydrofluoric acid (HF, J. T. Baker Chemical Co.) for 4 days at 4 °C (23). HF was removed by 4 or 5 cycles of evaporation (Speed-Vac, Savant) followed by rehydration with distilled, deionized water. Evaporated material was resuspended in high performance liquid chromatography (HPLC) grade water (Burdick and Jackson) and passed through an ultrafiltration membrane (Centricon 3, Amicon). The filtrate was injected onto a C_{18} reverse-phase HPLC column (24) (4.6 mm × 25 cm, Zorbax, Dupont) mounted on a Hewlett-Packard 1090L chromatograph, and run isocratically in HPLC grade water (0.5 ml/min). Fractions were evaporated to dryness (Speed-Vac, Savant), and those fractions containing visible residue were spotted onto high performance thin-layer chromatography (HPTLC) plates. Hexasaccharide-containing fractions were pooled, evaporated, suspended in a mixture of acetonitrile and water (HPLC grade) (65:35), and applied to an 8 mm × 30-cm MicroPak AX-5 (Varian) diaminopropyl-bonded silica HPLC column (25). The hexasaccharide was eluted by passing a linear gradient of water through the column. The gradient was initiated after washing the column for 15 min with the initial acetonitrile:water mixture; the gradient was formed by increasing the aqueous phase with 1.75% water/min at a flow rate of 1 ml/min. Fractions were evaporated and assayed by HPTLC as above. For removal of leached column material (which gave an apparent increase in yield of recovered dry weight over injected material) and for enhancement of purity, hexasaccharide-containing fractions were dissolved in HPLC water and eluted with water (0.3 ml/min) from two Superose 12 (Pharmacia LKB Biotechnology Inc.) columns in series. Fractions were evaporated and assayed as above; hexasaccharide material was pooled for further analysis.

High Performance Thin-layer Chromatography—HPLC fractions were applied to Silica 60 HPTLC 10 × 10-cm glass-backed plates (EM Science, Cherry Hill, NJ), and resolved using a mobile phase consisting of chloroform:methanol:water in a ratio of 10:10:3 (by volume) (26). Constituents in the samples were visualized by spraying the plates with a freshly prepared solution of naphthoresorcinol (20 mg), sulfuric acid (0.2 ml), and ethanol (10 ml) (27).

Methylation Analysis and Butanolysis—Approximately 0.5 mg of the sample was pre-reduced in 0.5 ml of 10 mg/ml $NaBD_4$ in 1 M NH_4OH for 1 h at room temperature. The excess $NaBD_4$ was destroyed by a few drops of glacial acetic acid and the borate was removed by repeated evaporation with methanol:acetic acid (9:1, v/v) followed by methanol. The sample was dissolved in deionized water, treated with Dowex 50 H^+ resin, and lyophilized. Methylation was accomplished by the Hakomori procedure described by York *et al.* (28). Analysis of the partially methylated alditol acetate derivatives was performed on an HP5890/5970 gas chromatograph with a mass-selective detection (GC/MSD) system employing a 30-m SP2330 fused silica column (Supelco). The D and L configurations of the constituting monosaccharides were determined by butanolysis of the native hexasaccharide. The resulting (+)-2-butyl glycosides were trimethylsilylated and analyzed by GLC using a 30-m DB-1 column from J&W Scientific (28).

^{252}Californium Plasma Desorption Mass Spectrometry—Native, acetylated, or reduced and acetylated hexasaccharide was analyzed by ^{252}Californium plasma desorption mass spectrometry (PDMS). The ^{252}Cf plasma desorption spectrometer was constructed by Prof. A. A. MacFarlane of Texas A&M University and modified by L. K. Pannell and H. M. Fales (National Heart, Lung and Blood Institute). The accelerating voltage was 10 kV and the flight path 42 cm. Samples in methanol were applied to an aluminized Mylar film by electrospraying. Data was collected on a Perkin-Elmer 3220 computer for times indicated. Fifty to 100 μg of sample was acetylated with 200 μl of pyridine (Pierce Chemical Co.) and 400 μl of acetic anhydride (Baker), incubated 16 h at room temperature, and evaporated. Samples were pre-reduced as above.

Nuclear Magnetic Resonance Spectroscopy—A sample (14 mg) of the hexasaccharide repeating unit of the cell wall polysaccharide from *S. sanguis* H1 was subjected to NMR spectroscopic analysis. The sample was repeatedly dissolved in D_2O (Aldrich; 99.8 and 99.96 atom % D, respectively) at room temperature and pD 6, with intermediate lyophilization, and stored in a vacuum desiccator over P_2O_5. Immediately prior to NMR spectroscopic analysis, the sample was redissolved in 0.5 ml of D_2O (Cambridge Isotope Laboratories; 99.96 atom % D), and transferred into a 5-mm NMR tube (Wilmad; 535-PP).

NMR spectroscopy was performed on a Bruker AM-500 spectrometer interfaced with an Aspect-3000 computer. The probe temperature was kept at 27 °C. ^{1}H chemical shifts (δ) are expressed in parts/million downfield from internal 4,4-dimethyl-4-silapentane-1-sulfonate (DSS), but were actually measured by reference to internal acetone (δ 2.225 in D_2O at 27 °C) or free acetate (δ 1.908 in D_2O at pD 6–8 and 27 °C), with an accuracy of 0.002 ppm. ^{13}C chemical shifts are expressed in parts/million downfield from internal DSS, with an accuracy of 0.02 ppm.

Two-dimensional (^{1}H,^{1}H) COSY spectroscopy was performed in the absolute-value mode (29) using a spectral width of 2400 Hz. The evolution time (t_1) was incremented in steps of 416 μs to obtain 256 free induction decays (f.i.d.), each consisting of the sum of 64 transients acquired in 2 K data points. Two-dimensional (^{1}H,^{1}H) Hartmann-Hahn (HOHAHA) spectroscopy was performed using the MLEV-17 sequence (30) during the isotropic mixing period (200 ms), incrementing t_1 in steps of 476 μs to obtain 512 f.i.d., each consisting of the sum of 64 transients acquired in 2 K data points. The spectral width was 1050 Hz. The strength of the spinlock field was 7.5 kHz. Quadrature detection in t_1 was accomplished by the time-proportional phase increment (TPPI) method (31).

A ^{13}C-detected (^{13}C,^{1}H) one-bond shift correlation (HETCOR) experiment was conducted (32), using a spectral width of 6250 Hz in the ^{13}C domain, incrementing t_1 in steps of 400 μs to obtain 32 f.i.d., each consisting of the sum of 1000 transients acquired in 2 K data points. A ^{1}H-detected (^{1}H,^{13}C) one-bond shift correlation (HMQC) spectrum was recorded in the absolute-value mode as described by Bax and Subramanian (33) using a ^{1}H spectral width of 1250 Hz, incrementing t_1 in steps of 60 μs to obtain 128 f.i.d. each consisting of the sum of 200 transients acquired in 2 K data points. The ^{1}H magnetization of protons attached to ^{12}C was suppressed solely by phase-cycling of pulses and receiver. ^{13}C decoupling during acquisition (t_2) was accomplished using the GARP pulse sequence (34). ^{1}H-detected (^{1}H,^{13}C) multiple-bond correlation (HMBC) spectroscopy was performed as described (35) with delays Δ_1 and Δ_2 set to 3.33 and 80 ms, respectively, using a ^{1}H spectral width of 1250 Hz, incrementing t_1 in steps of 60 μs to obtain 200 f.i.d., each consisting of the sum

of 400 transients acquired in 2 K data points. The ^{1}H-detected (^{1}H,^{13}C) shift correlation experiments (HMQC and HMBC) utilized a 5-mm broad-band probe with reversed geometry. The decoupler transmitter was used for ^{1}H pulses (reverse mode) and the sample was not spun (compare Refs. 36 and 37).

RESULTS

Hexasaccharide Purification—By modifying our purification procedure published previously (16), and using three separate HPLC techniques, 16 mg of highly purified hexasaccharide was obtained from the cell wall polysaccharide of *S. sanguis* H1 for further analysis.

Determination of Glycosyl Composition and Linkage Positions—Composition analysis had shown (16) that the repeating oligosaccharide unit consists of Rha, Gal, and Glc in the molar ratio of 2:3:1. The absolute configurations of the glycosyl residues were determined by preparing the (+)-2-butyl glycosides (28, 37). GLC analysis of the trimethylsilylated butyl glycosides showed that the rhamnosyl residues were in the L configuration, while the other glycosyl residues were all D.

Methylation analysis of the oligosaccharide showed it to consist of terminal Rha, 2-linked Rha, 3-linked Gal, 4-linked Glc, and 3-linked reducing Gal (Gal^R), in the ratio of 1:1:2:1:1, by virtue of the mass spectra and retention times of the resulting partially methylated alditol acetates (PMAA). The galactosyl residue at the reducing end was identified by GC/MSD analysis of the PMAA derived from the oligosaccharide which was prereduced with $NaBD_4$. This procedure resulted in a 3-*O*-acetyl-1,2,4,5,6-penta-*O*-methyl-hexitol (galactitol) with a deuterium atom at C1.

^{252}Cf-Plasma Desorption Mass Spectrometry—PDMS of the native repeating oligosaccharide unit verified gas chromatographic evidence (16) that the oligosaccharide was a hexasaccharide. The mass of the molecule was 958.9 (C = 12.01115), which corresponds to $C_{38}H_{62}O_{29}$ as derived from the PDMS spectrum which showed an $(M + Na)^+$ ion at *m/z* 982. The peracetylated hexasaccharide showed a *m/z* value of 1716 for the $(M + H)^+$ ion, indicating the presence of 18 acetylated hydroxyl groups ($C_{72}H_{98}O_{47}$ = 1715.6). These data are consistent with the hexasaccharide being $Hex_4[dHex]_2$. In addition, sequence information became available from the spectrum of the peracetylated hexasaccharide (*cf.* Ref. 38). Fragmentation occurred in several places within the structure providing acylium ions via cleavage at the protonated acetal linkages, as follows:

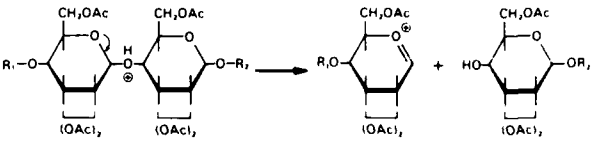

STRUCTURE 1

The pertinent ions are summarized above the spectrum in Fig. 1. The number of acetyl groups shown in each peak was determined from the mass spectrum of a perdeuterioacetylated sample and confirms the ion structures shown. From the fragment at *m/z* 503, it was deduced that the 2 Rha (dHex) residues were attached to each other, at the nonreducing end of the hexasaccharide. The peak at *m/z* 1368 expressing the cleavage of the reducing end hexose from the hexasaccharide acetate is surprisingly weak. In its place is a rather strong peak at *m/z* 620 that must result from cleavage of a fragment containing the last two hexoses, in the "opposite" direction, as follows:

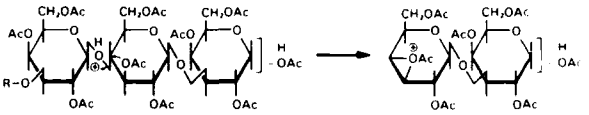

STRUCTURE 2

Conceivably, this cleavage results from anchimeric assistance from the *trans*-oriented 3-acetate of the penultimate glucose (see below) moiety. The same stereochemical consequences would also hold for a penultimate galactose linked at the 3-position which would be expected to undergo cleavage assisted by its *trans* 2-acetate. The presence of a hexose (galactose) residue at the reducing end was confirmed by comparing the spectrum of the acetylated hexasaccharide (Fig. 1) to the spectrum of the pre-reduced ($NaBH_4$), acetylated hexasaccharide (not shown). Signals at *m/z* 331 and 620 were no longer

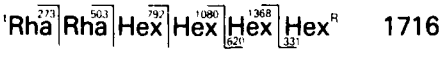

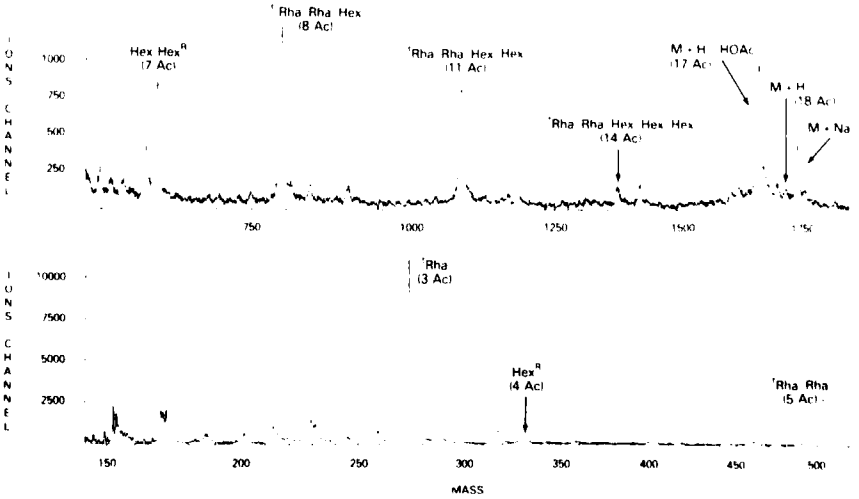

FIG. 1. **^{252}Cf-Plasma desorption mass spectrum of the HPLC-purified, acetylated repeating oligosaccharide.** The *m/z* value (1716) for the parent ion $(M + H)^+$ indicates that the oligosaccharide is a hexasaccharide consisting of 2 deoxyhexose (rhamnose) and 4 hexose (glucose and galactose) residues, corresponding to a mass of 959 for the native hexasaccharide. Other *m/z* values and peaks denote fragments of the parent ion.

present, whereas signals at m/z 375 and 664 appeared in the latter spectrum. Signals at m/z 273, 503, 792, and 1080 were prominent in both spectra. The combined results from chemical and mass spectrometric analyses indicate that the structure of the hexasaccharide is L-Rha*p*(1→2)L-Rha*p*→D-Hex*p*→D-Hex*p*-D-Hex*p*(1→3)D-Gal in which two D-Hex are galactosyl residues and the third is a glucosyl residue.

Completion of Primary Structure Determination by ^1H and ^{13}C NMR Spectroscopy—The ^{1}H NMR spectrum of the hexasaccharide (Fig. 2*A*) shows seven anomeric resonances. Based on the chemical shifts and coupling constants, four of these resonances, δ 5.18 (J_{12} = 3.7 Hz), δ 5.10 (J_{12} = 1.8), δ 5.06 (J_{12} = 3.0), and δ 4.88 (J_{12} = 1.9) were tentatively assigned to H1 of α-linked glycosyl residues. The remaining three resonances, δ 4.6, δ 4.53 (J_{12} = 7.9) and δ 4.42 (J_{12} = 7.9), were assigned to H1 of β-linked glycosyl residues. The relatively low intensities of the resonances at δ 5.18 and δ 4.53 (relative areas of 0.3 and 0.6, respectively, compared to 1.0 for all the other anomeric resonances) suggest that they were due to the H1 atoms of the α- and β-anomers of the reducing galactosyl residue, respectively. The signal at δ 4.6 which appears as a set of three peaks consists actually of two doublets, δ 4.61 (J_{12} = 8.6) and δ 4.60 (J_{12} = 8.6). The two doublets (intensity ratio 1:2) were assigned to the H1 of the hexosyl residue that is linked to the reducing galactosyl residue and were attributed to the α/β-anomerization of this reducing galactosyl residue. This assignment is based on the HMQC and HMBC experiments which are discussed below. The doublet at δ 4.61 occurs when this hexosyl residue is linked to the α-anomer and the other doublet, at δ 4.60, occurs when it is linked to the β-anomer of the reducing galactose residue. The resonances at δ 5.10 and δ 4.88 can be assigned to the 2 rhamnosyl residues by virtue of their small J_{12} coupling constants. That these rhamnosyl residues were involved in α-glycosyl linkages was confirmed by recording a ^{1}H-coupled ^{13}C spectrum of the hexasaccharide (see below). Henceforth, we will use the anomeric proton assignments to distinguish between the seven ^{1}H NMR spin systems, as follows: the resonances at δ 5.18 and δ 4.53 being assigned to the H1 of the α- and β-anomer of the reducing galactosyl residue, these were denoted α-^{R}Gal$_{5.18}$ and β-^{R}Gal$_{4.53}$; the 2 rhamnosyl residues were denoted α-Rha$_{5.10}$ and α-Rha$_{4.88}$. The doublet at δ 4.42 and the two doublets at δ 4.61 and δ 4.60 were assigned to two β-linked hexosyl residues, β-Hex$_{4.42}$ and β-Hex$_{4.6}$, respectively, while

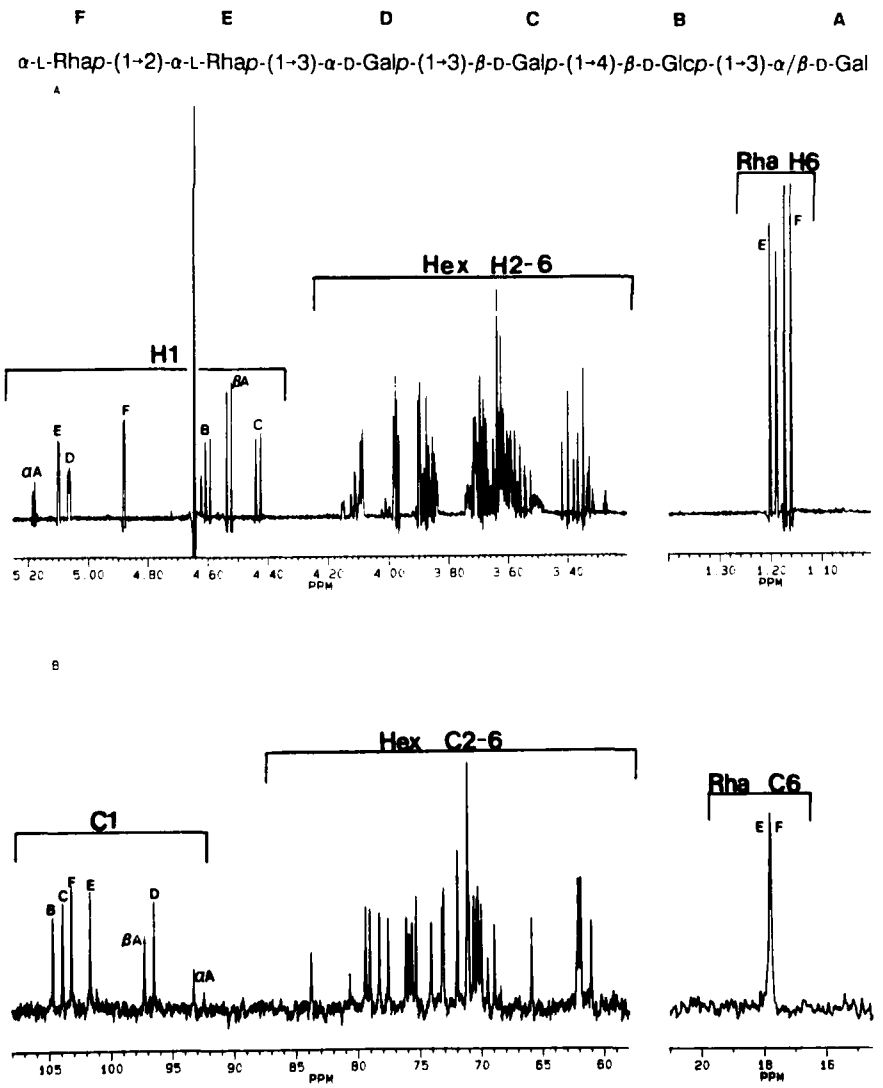

FIG. 2. **One-dimensional ^{1}H and ^{13}C NMR spectra of the HPLC-purified hexasaccharide from the *S. sanguis* H1 polysaccharide.** 500 MHz ^{1}H NMR (*A*) and 125 MHz ^{13}C NMR spectrum (*B*) of 14 mg of material in D_2O at 27 °C and pD 6.

the remaining resonance at δ 5.06 is assigned to an α-linked hexosyl residue, α-$Hex_{5.06}$.

Further ^1H assignments for each glycosyl residue were determined by the combination of two-dimensional (^1H,^1H) correlation spectroscopy (COSY), and homonuclear Hartmann-Hahn (HOHAHA) spectroscopy (see Fig. 3). The results are explained below and are compiled in Table I.

With regard to the rhamnosyl residues, the COSY experiment showed that α-$Rha_{5.10}$ H1 is coupled to H2 at δ 3.97 and that α-$Rha_{4.88}$ H1 is coupled to H2 at δ 3.96. Coupling was also observed between the H6 methyl protons at δ 1.20 and H5 at δ 3.71, and between H6 methyl protons at δ 1.18 and H5 at δ 3.62. This information, together with the HOHAHA results, allowed the complete assignment of the ^1H subspectra of both rhamnosyl residues. In the case of α-$Rha_{5.10}$, the HOHAHA subspectrum across the H1 resonance at δ 5.10 (Fig. 3) showed, in addition to the H2 multiplet of narrow width (<9 Hz) at δ 3.97, a doublet of doublets at δ 3.87, a multiplet at δ 3.71, and a doublet of doublets at δ 3.40. The narrow width of the H2 doublet of doublets (δ 3.97) is due to the small coupling constants resulting from the equatorial-equatorial relationship of H2 to H1 and its equatorial-axial relationship to H3. The doublet of doublets at δ 3.89 can be assigned to H3 (J_{23} = 5 Hz, J_{34} = 10 Hz). The doublet of doublets at δ 3.40 appears as a triplet and can be assigned to H4 ($J_{34} = J_{45}$ = 10 Hz). The relatively large coupling constants reflect the diaxial relationship of H4 with both H3 and H5. The multiplet at δ 3.71 is assigned to H5 in accordance with the COSY experiment (see above). Since the COSY experiment also showed that H5 at δ 3.71 is coupled to the H6 protons at δ 1.20, the ^1H assignment of α-$Rha_{5.10}$ was completed. The complete ^1H assignment of α-$Rha_{4.88}$ was made in an analogous manner.

With respect to the reducing galactosyl residue, the α-$^RGal_{5.18}$ H2 signal was assigned from the COSY experiment at δ 3.88 due to its cross peak to H1 at δ 5.18. The HOHAHA subspectrum across H1 at δ 5.18 (Fig. 3) shows multiplets at δ 3.88, 3.86, and 4.15. The multiplet at δ 4.15 is assigned to H4. Its relatively downfield position and narrow peak width (<7 Hz) is typical for an equatorial Gal H4 proton which has an equatorial-axial relationship with both H3 and H5. Thus, the remaining multiplet at δ 3.86 is assigned to H3. The subspectrum through H1 does not allow assignment of H5 from α-$^RGal_{5.18}$, because of the inefficiency of magnetization transfer from H4 to H5 (J_{45} < 1.5 Hz) (36). However, the subspectrum through δ 4.15 revealed an additional multiplet

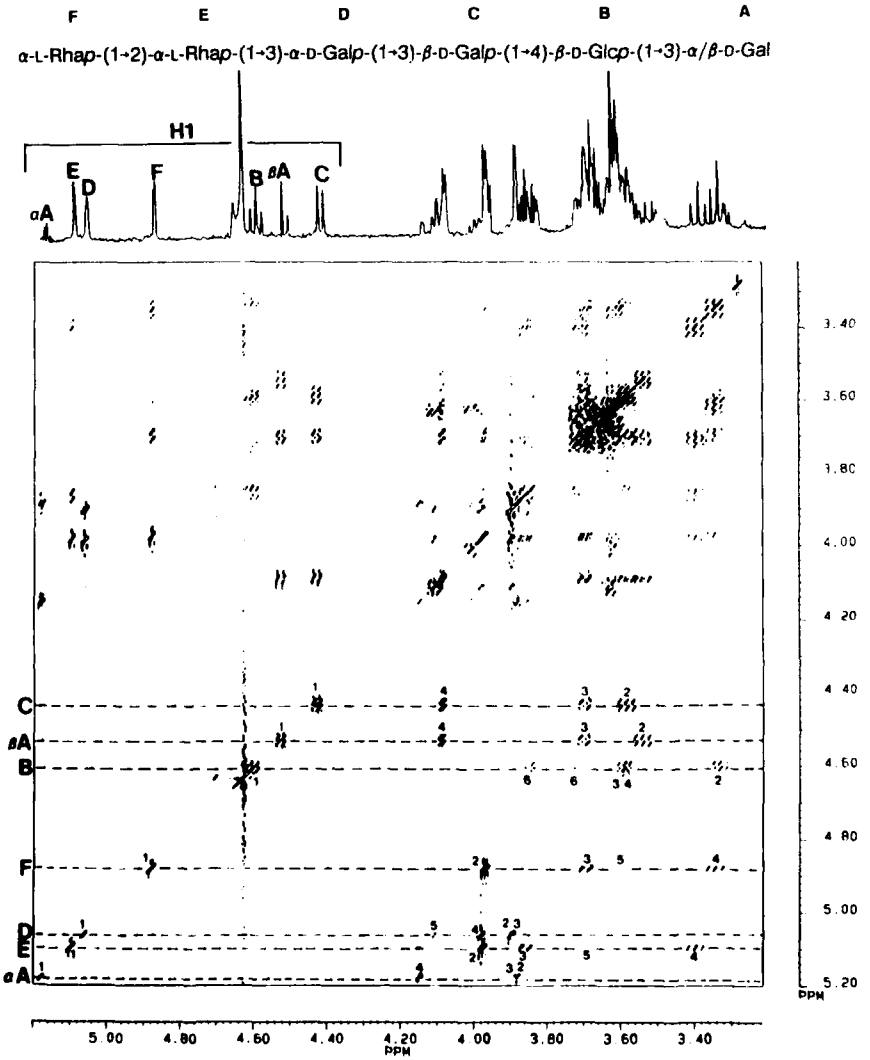

FIG. 3. **Two-dimensional HOHAHA spectrum of the hexasaccharide isolated from the cell wall polysaccharide of *S. sanguis* H1.** The structure of the compound and its one-dimensional ^1H spectrum are shown on *top* of the contour map. *Horizontal, dashed lines* through the anomeric proton resonances on the diagonal constitute the subspectra of the glycosyl residues of the hexasaccharide. The numbers correspond to the location of the protons in the ring. The HOHAHA spectrum was obtained at 500 MHz, on 14 mg of the oligosaccharide in D_2O, 27 °C, pD 6; total measuring time: 10 h. Data matrix: 512 × 2048; 64 scans/t_1 value; spin locking by MLEV-17; mixing time 200 ms; quadrature detection in t_1 by TPPI; sine-bell window functions applied in both dimensions prior to Fourier transformation.

TABLE I

^{1}H and ^{13}C NMR chemical shifts for the constituent residues of the repeating hexasaccharide from the cell wall polysaccharide of S. sanguis H1

Data were acquired at 500 MHz (^{1}H) and 125 MHz (^{13}C), for a neutral solution of the hexasaccharide in D_2O at 27 °C.

Residue[a]	H1 C1	H2 C2	H3 C3	H4 C4	H5 C5	H6 C6
α-Gal$_{5.18}$	5.18	3.88	3.86	4.15	4.00	3.58–3.65[b]
(αA)	93.3	69.0	80.8	70.1	71.2	62.0[c]
β-Gal$_{4.53}$	4.53	3.54	3.70	4.09	3.62	3.58–3.65[b]
(βA)	97.3	72.0	83.8	69.5	75.9	62.0[c]
β-Glc$_{4.6}$	4.60, 4.61	3.33	3.58	3.58	3.50	3.72, 3.85
(B)	104.8	74.1	75.4	79.4	75.7	61.1
β-Gal$_{4.42}$	4.42	3.58	3.70	4.09	3.63	3.58–3.65[b]
(C)	104.0	70.6	78.4	66.0	76.2	61.9[c]
α-Gal$_{5.06}$	5.06	3.90	3.90	3.99	4.11	3.71, 3.62
(D)	96.5	69.0	77.6	70.5	72.0	62.1[c]
α-Rha$_{5.10}$	5.10	3.97	3.87	3.40	3.71	1.20
(E)	101.8	79.1	71.5	73.2	70.4	17.5
α-Rha$_{4.88}$	4.88	3.96	3.69	3.34	3.62	1.18
(F)	103.3	71.1	71.2	73.2	70.4	17.5

[a] Residues are denoted by capital letters A–F, indicating their sequence in the hexasaccharide (compare to Fig. 2); the subscripts indicate the chemical shifts of their anomeric protons.

[b] These ^{1}H resonances could not be assigned from the HOHAHA spectrum (Fig. 3); their assignment is based on the C-H correlation spectra.

[c] The assignments of these carbon resonances may be interchanged.

at δ 4.00 which was assigned to H5. Similarly, the H2 resonance for β-^{R}Gal$_{4.53}$ was assigned from the COSY experiment at δ 3.54 because of its cross-peak to H1 at δ 4.53. In addition, the HOHAHA subspectrum across the H1 at δ 4.53 showed multiplets at δ 4.09 and 3.70 (see Fig. 3). The multiplet at δ 4.09 has a narrow peak width (<8 Hz) and is assigned to H4. The remaining resonance at δ 3.70 is assigned to H3. A subspectrum through δ 4.09 reveals an additional multiplet of lower intensity at δ 3.62 which is assigned to H5.

The H2 of β-Hex$_{4.42}$ resonates at δ 3.58 as determined from the COSY experiment. The HOHAHA subspectrum through δ 4.42 shows additional multiplets at δ 4.09 and δ 3.70 (see Fig. 3). The identity of the Hex residue can be determined from the set of vicinal coupling constants of its protons, as follows. The multiplet at δ 4.09 has a total width of <8 Hz. This narrow peak width, its chemical shift, together with the knowledge of the glycosyl composition, identify it as the H4 of a galactosyl residue. Thus, β-Hex$_{4.42}$ is a galactosyl residue, β-Gal$_{4.42}$. The remaining multiplet at δ 3.70 is assigned to H3 of this residue. As with the β-^{R}Gal$_{4.53}$ residue, the small value for J_{45} prohibits the appearance of H5, H6, and H6′ signals in the HOHAHA subspectrum through H1 at δ 4.42. However, the HOHAHA subspectrum across δ 4.09 shows an additional multiplet at δ 3.63 which is assigned to H5. The coupling constants, obtained from the one-dimensional ^{1}H spectrum and the HOHAHA subspectra are: J_{12} (7.9 Hz), J_{23} (11.3 Hz), J_{34} (3.1 Hz), and J_{45} (1.0 Hz). These coupling constants and the chemical shifts for H1–H5 are consistent with the β-Hex$_{4.42}$ residue being a galactopyranose group.

The α-Hex$_{5.06}$ H2 resonance was assigned from the COSY spectrum at δ 3.90. The HOHAHA subspectrum through δ 5.06 (Fig. 3), showed, in addition to the H2 resonance, a multiplet at δ 3.99 which has a narrow width (<5 Hz). Its downfield position and narrow peak width are characteristic for H4 of a galactosyl residue. Thus, the α-Hex$_{5.06}$ is the remaining galactosyl residue, α-Gal$_{5.06}$. The multiplet at δ 3.90, observed in the HOHAHA subspectrum, is assigned to the coresonant H2 and H3 atoms. It should be mentioned that the chemical shifts of the H2 and H3 resonances for the α-^{R}Gal$_{5.18}$ residue described above (δ 3.88 and 3.86, respectively) were also very similar to one another. The HOHAHA subspectrum through δ 3.99 shows an additional multiplet at δ 4.11 and two multiplets of lower intensity at δ 3.71 and 3.62. The resonance at δ 4.11 is assigned to H5, based on its chemical shift (39). The remaining resonances at δ 3.71 and 3.62 are assigned to H6 and H6′.

Since we have accounted for 2 rhamnosyl and 3 galactosyl residues, the remaining hexosyl residue, β-Hex, in which the anomeric proton resonates as two doublets around δ 4.6 (δ 4.61 and 4.60), must be glucose, β-Glc (J_{12} = 8.6 Hz). The COSY experiment showed that the H2 resonance of this residue is at δ 3.33. The HOHAHA subspectrum through δ 4.60 (Fig. 3) showed additional broad multiplets at δ 3.85, 3.72, 3.58, and 3.50. Typically, the set of relatively large vicinal coupling constants allows magnetization transfer in the glucosyl residue from H1 all the way to H6 and H6′ during the mixing period of the HOHAHA experiment. The multiplet at δ 3.58 is particularly broad (40 Hz) and is also the most intense. The multiplet at δ 3.50 is the least intense. The multiplets at δ 3.85 and 3.72 appear to be two doublets of doublets and their chemical shifts and coupling constants ($J_{66'}$ = −12 Hz) are consistent with the H6 protons of a β-glucosyl residue. The broad, intense multiplet at δ 3.58 is due to two coresonant protons, namely H3 and H4. The remaining multiplet at 3.50 is assigned to H5. This assignment is also confirmed by the COSY experiment in which the H6 protons were coupled to the H5 proton at δ 3.50.

Once the ^{1}H spectrum of the hexasaccharide had been assigned, the ^{13}C spectrum was assigned both by a ^{1}H-detected, as well as by a ^{13}C-detected one-bond (^{1}H,^{13}C) shift correlation experiment (HMQC and HETCOR, respectively). Both spectra showed one-to-one correlations between carbons and the proton(s) that is (are) directly attached to it; the HMQC spectrum has relatively high resolution in the ^{1}H dimension, while the HETCOR spectrum shows better resolution in the ^{13}C domain. The one-dimensional ^{13}C spectrum of the hexasaccharide is shown in Fig. 2*B*; the derived ^{13}C assignments for the hexasaccharide are included in Table I. In instances where two or more protons had the same chemical shift, it was not possible to make the ^{13}C assignment directly from the $^1J_{C-H}$ correlation spectra. For example, the H3s of β-^{R}Gal$_{4.53}$ and β-Gal$_{4.42}$ both resonate at δ 3.70. The resonances for the C3s of these 2 galactosyl residues could be distinguished, however, since the C-H cross-peaks of the reducing galactosyl residue were consistently of lower intensity than the other cross-peaks. Thus, the cross-peak at δ 83.8/δ 3.70 (which was of lower intensity), and that at δ 78.4/δ 3.70 were assigned to the C3s of β-^{R}Gal$_{4.53}$ and β-Gal$_{4.42}$, respectively. The C4s of these 2 residues were similarly assigned, based on relative intensity of cross-peaks, since their H4s both resonate at δ 4.09. The H3 and H4 of β-Glc$_{4.6}$ and the H2 of β-Gal$_{4.42}$ all resonate at δ 3.58. Connectivities to ^{13}C signals at δ 79.4, δ 75.4 and δ 70.6 are observed. The signal at δ 79.4 was assigned to C4 of β-Glc since methylation data showed that the glucosyl residue is linked at position 4 (see above) and, therefore, this carbon would be shifted furthest downfield. The literature (40) reports that the C3 resonance of a β-glucosyl residue is consistently found downfield from the C2 of a β-galactosyl residue and, thus, the peaks at δ 75.4 and δ 70.6 were assigned to the C3 of Glc, and C2 of β-Gal$_{4.42}$, respectively. Both the H2 and H3 of α-Gal$_{5.06}$ resonate at δ 3.90. Since methylation data show that all the galactosyl residues are linked at position 3 the resonance at δ 77.6 was assigned to C3 and that at δ 69.0 was assigned to C2. Finally, the H5s of β-^{R}Gal$_{4.53}$ and α-Rha$_{4.88}$ both resonate at δ 3.62. The literature (40) shows that

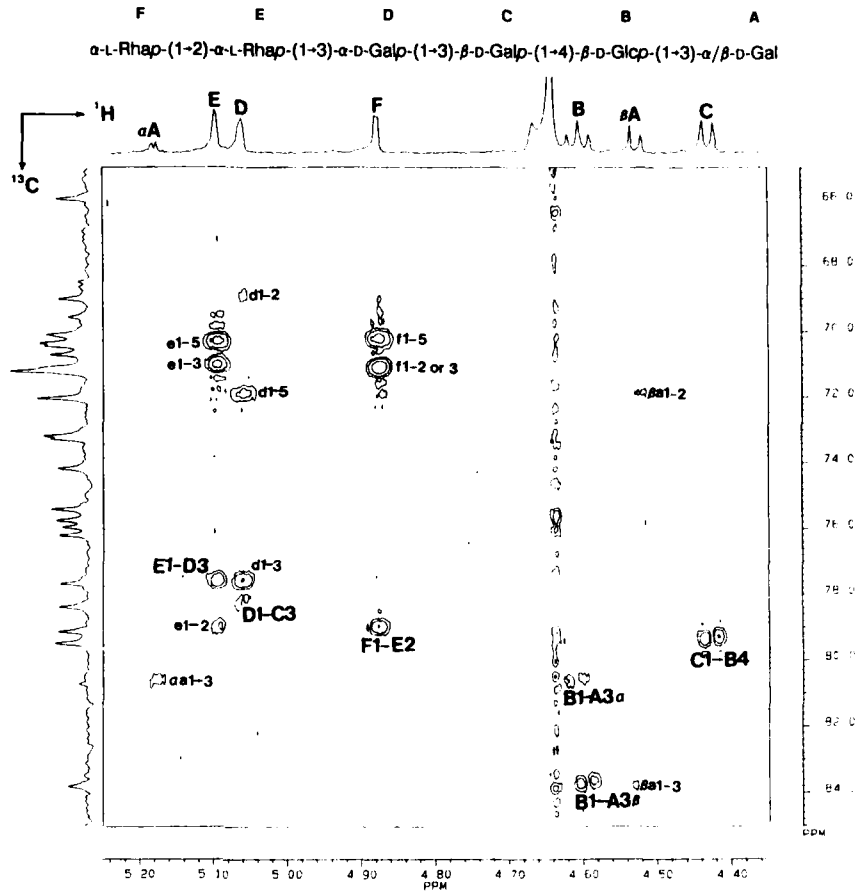

FIG. 4. **Heteronuclear multiple-bond correlation (HMBC) spectrum of the hexasaccharide isolated from the cell wall polysaccharide of *S. sanguis* H1.** The selected region shows the long-range ^{1}H-^{13}C connectivities of the anomeric protons. The structure of the compound and its one-dimensional ^{1}H spectrum are shown on *top* of the contour map; the ^{13}C projection is shown alongside the *vertical axis*. Cross-peaks marked by *capital letters* indicate three-bond couplings ($^3J_{CH}$) across the glycosidic linkages between pertinent residues; those marked by *small letters* refer to $^2J_{CH}$ and $^3J_{CH}$ couplings within the glycosyl rings. The HMBC spectrum was obtained at 500 MHz, on 14 mg of the oligosaccharide in D_2O, 27 °C, pD 6; total measuring time: 40 h. Data matrix: 200 × 2048; 400 scans/t_1 value; squared sine-bell multiplication applied in the ^{1}H dimension. Gaussian line broadening in the ^{13}C dimension, prior to Fourier transformation.

TABLE II

Multiple-bond connectivities between the anomeric protons of the constituent glycosyl residues and carbon atoms within the glycosyl residues and across the glycosidic bonds, as observed for the repeating hexasaccharide unit of S. sanguis H1 cell wall polysaccharide

Cross-peak	Coordinates		Connectivity between		
	δ ^{1}H	δ ^{13}C	H1 of	C-atom	Residue
αa1-3	5.18	80.8	α-^{R}Gal$_{5.18}$	C3	α-^{R}Gal$_{5.18}$
βa1-2	4.53	72.0	β-^{R}Gal$_{4.53}$	C2	β-^{R}Gal$_{4.53}$
βa1-3	4.53	83.8	β-^{R}Gal$_{4.53}$	C3	β-^{R}Gal$_{4.53}$
d1-2	5.06	69.0	α-Gal$_{5.06}$	C2	α-Gal$_{5.06}$
d1-3	5.06	77.6	α-Gal$_{5.06}$	C3	α-Gal$_{5.06}$
d1-5	5.06	72.0	α-Gal$_{5.06}$	C5	α-Gal$_{5.06}$
e1-2	5.10	79.1	α-Rha$_{5.10}$	C2	α-Rha$_{5.10}$
e1-3	5.10	71.5	α-Rha$_{5.10}$	C3	α-Rha$_{5.10}$
e1-5	5.10	70.4	α-Rha$_{5.10}$	C5	α-Rha$_{5.10}$
f1-2 or 3	4.88	71.2	α-Rha$_{4.88}$	C2 and/or C3	α-Rha$_{4.88}$
f1-5	4.88	70.4	α-Rha$_{4.88}$	C5	α-Rha$_{4.88}$
F1-E2	4.88	79.1	α-Rha$_{4.88}$	C2	α-Rha$_{5.10}$
E1-D3	5.10	77.6	α-Rha$_{5.10}$	C3	α-Gal$_{5.06}$
D1-C3	5.06	78.4	α-Gal$_{5.06}$	C3	β-Gal$_{4.42}$
C1-B4	4.42	79.4	β-Gal$_{4.42}$	C4	β-Glc$_{4.6}$
B1-A3α	4.61	80.8	β-Glc$_{4.6}$	C3	α-^{R}Gal$_{5.18}$
B1-A3β	4.60	83.8	β-Glc$_{4.6}$	C3	β-^{R}Gal$_{4.53}$

[a] Connectivities observed in the HMBC spectrum of the hexasaccharide (see Figure 4). Bold capital letters indicate $^3J_{CH}$ couplings across the glycosidic bonds; bold small letters indicate $^2J_{CH}$ and $^3J_{CH}$ couplings within a glycosyl ring.

the C5 of a β-galactosyl residue is consistently found downfield from that of an α-rhamnosyl residue and, therefore, the resonances at δ 75.9 and δ 70.4 are assigned to β-^{R}Gal$_{4.53}$ and α-Rha$_{4.88}$, respectively. Both the proton and carbon assignments for H6 and C6 of α-^{R}Gal$_{5.18}$, β-^{R}Gal$_{4.53}$, and β-Gal$_{4.42}$ were estimated from the HMQC and HETCOR spectra since these H6 assignments could not be made from the HOHAHA experiment.

The glycosidic linkages of the rhamnosyl residues were confirmed to have the α-configuration, by recording a ^{1}H-coupled ^{13}C spectrum of the hexasaccharide. From this spectrum, the J_{CH} values for the α-Rha$_{5.10}$ and α-Rha$_{4.88}$ C1s (δ 101.8 and 103.3, respectively) were determined to be 171.7 and 170.2 Hz, respectively (40). The ring sizes of all glycosidically linked residues were confirmed to be pyranoses; notably, the absence of anomeric ^{13}C-signals around δ 110 ppm (Fig. 2*B*) points to the linked Gal residues being in the pyranose ring structure (see below).

Once the ^{1}H and ^{13}C spectra had been virtually completely assigned, the sequence of the glycosyl residues in the hexasaccharide was determined by a heteronuclear multiple bond correlation (HMBC) experiment. In this experiment, interglycosidic couplings ($^3J_{CH}$) of the anomeric protons across the glycosyl oxygen to the linked carbon were observed. In addition, intra-ring couplings of the anomeric proton to C3 ($^3J_{CH}$) and in some cases to C2 ($^2J_{CH}$) and C5 ($^3J_{CH}$) were observed. Fig. 4 shows the portion of the HMBC spectrum used for sequencing, and Table II lists the intra- and inter-ring long-range C-H connectivities of the anomeric protons. The se-

quence of the hexasaccharide was deduced from the couplings across the glycosidic bonds observed in the HMBC spectrum, together with the assignments given in Table I, as follows: The H1 doublet at δ 4.60 is coupled to the ^{13}C resonance at δ 83.3 (C3 of β-^{R}Gal$_{4.53}$), while the other Glc H1 doublet at δ 4.61 is coupled to the ^{13}C signal at δ 80.8, which is C3 of the α-^{R}Gal$_{5.18}$ indicating that the β-Glc residue is linked to C3 of ^{R}Gal. Thus the sequence at the reducing end of the hexasaccharide is →-β-Glc-(1→3)-α/β-Gal. The H1 doublet at δ 4.42 is coupled to the ^{13}C resonance at δ 79.4 and shows that the β-Gal$_{4.42}$ is linked to the C4 of Glc. The H1 signal at δ 5.06 shows an interglycosidic coupling to the ^{13}C signal at δ 78.4, indicating that α-Gal$_{5.06}$ is linked to the C3 of β-Gal$_{4.42}$. Therefore, the tetrasaccharide at the reducing end of the hexasaccharide structure is: →-α-Gal-(1→3)-β-Gal-(1→4)-β-Glc-(1→3)-α/β-Gal. The H1 at δ 5.10 is coupled to the ^{13}C resonance at δ 77.6 showing that α-Rha$_{5.10}$ is linked to the C3 of α-Gal$_{5.06}$. Finally, H1 at δ 4.88 is coupled to the ^{13}C signal at δ 79.1 showing that α-Rha$_{4.88}$ is linked to the C2 of α-Rha$_{5.10}$. Thus, the complete primary structure of the hexasaccharide, including the absolute stereochemical configurations and ring sizes of the residues, is as follows: α-L-Rha*p*-(1→2)-α-L-Rha*p*-(1→3)-α-D-Gal*p*-(1→3)-β-D-Gal*p*-(1→4)-β-D-Glc*p*-(1→3)-α/β-D-Gal.

The sequence and linkage positions, as determined by HMBC NMR spectroscopy, are in full agreement with the PDMS and methylation data described above.

DISCUSSION

The complete primary structure of the hexasaccharide repeating unit from *S. sanguis* H1 cell wall polysaccharide has been elucidated by a combination of two-dimensional homonuclear (COSY and HOHAHA) and heteronuclear (HMQC and HMBC) NMR experiments, in conjunction with PDMS and chemical analyses. Given that the oligosaccharide consists of Rha, Gal, and Glc residues in the ratio of 2:3:1, methylation analysis of the deuterio-reduced hexasaccharide showed that a Gal residue is at the reducing end, and PDMS revealed the compound to be a linear hexasaccharide containing the L-Rha-(1→2)-L-Rha moiety at the nonreducing end.

PDMS technology has become available relatively recently; the technique has since been used for a variety of molecules, including small proteins, peptides, glycolipids and phospholipids (41). To our knowledge this is the first report to utilize PDMS for deriving structural information of a previously uncharacterized oligosaccharide. Fast atom bombardment (FAB) mass spectrometry has been used extensively for oligosaccharide characterization (42). However, interference from glycerol adducts and from matrix polymerization is common in FAB spectra. We believe that PDMS offers a viable alternative to FAB due to lack of such matrix effects.

The sequence of the constituent glycosyl residues, including the configurations of the glycosidic linkages, the ring sizes and the glycosyl linkage positions, was deduced by the aforementioned NMR techniques. To accomplish this, the virtually complete assignment of the ^{1}H and ^{13}C NMR spectra of the hexasaccharide was necessary. With respect to the anomeric linkage configurations it should be mentioned that, since L-Rha*p* occurs in the $^{1}C_{4}$ conformation, with H2 in equatorial orientation, neither the H-1 and C-1 chemical shifts nor the coupling constants $^{3}J_{H1H2}$ were useful in determining the configuration of the linkages (39, 40). Evidence for the α-configurations was obtained from the $^{1}J_{C1H1}$ values (40).

Once the ^{1}H and ^{13}C spectra of the hexasaccharide had been assigned by the combination of COSY, HOHAHA, and HETCOR/HMQC experiments, the key experiment to sequence the hexasaccharide was the HMBC experiment. Long-range, $^{3}J_{CH}$ couplings between anomeric protons and substituted carbon atoms across the glycosidic linkages allowed the linkage positions and the entire sequence to be determined. To date, the integrated approach of COSY/HOHAHA and HMQC/HMBC NMR spectroscopy has been applied to sequencing carbohydrates, at the level of small oligosaccharides (43, 37), larger oligosaccharides (36, 17), as well as for polysaccharides (44). To be able to use this strategy successfully, a minimum of 3–5 μmol of carbohydrate are required. The most elegant aspect of the approach is its use of scalar couplings only; this leaves dipolar connectivities to be used for conformational analysis (36, 45).

The structure of the *S. sanguis* H1 hexasaccharide is contrasted to the *S. sanguis* 34 hexasaccharide in that two GalNAc and a galactofuranose residue are present in the latter structure. The complete structure of the *S. sanguis* 34 hexasaccharide has been reported (46) as: α-D-Gal*p*NAc-(1→3)-β-L-Rha*p*-(1→4)-β-D-Glc*p*-(1→6)-β-D-Gal*f*-(1→6)-β-D-Gal*p*-NAc-(1→3)-D-Gal. A recent report (17) gave the structure of the *S. sanguis* strain J22 polysaccharide repeating unit, this being a heptasaccharide. The core structure is a hexasaccharide very similar to the *S. sanguis* 34 hexasaccharide, with an additional Rha. The strain J22 structure was reported as:

$$\begin{array}{l} \alpha\text{-D-Gal}p\text{NAc-}(1\to3)\text{-}\beta\text{-L-Rha}p\text{-}(1\to4)\text{-}\beta\text{-D-Glc}p\text{-}(1\to6)\text{-} \\ \qquad\qquad\qquad\qquad\qquad\qquad\qquad\qquad\qquad\qquad\qquad\qquad \nearrow \\ \qquad\qquad\qquad\qquad\qquad\qquad\qquad\qquad\qquad\qquad\qquad\qquad \alpha\text{-L-Rha}p\text{-}(1\to2)\text{-} \\ \qquad\qquad\qquad\qquad\qquad\qquad\qquad\qquad\qquad\qquad\qquad\qquad \beta\text{-D-Gal}f\text{-}(1\to6)\text{-}\beta\text{-D-Gal}p\text{-}(1\to3)\text{-D-GalNAc.} \end{array}$$

The three *S. sanguis* strains, H1, 34, and J22 coaggregate with the same actinomyces partners (primary colonizers), but appear to utilize adhesin-to-polysaccharide receptor mechanisms in different ways (47). To establish cell-to-cell contact and maintain the aggregated state in these streptococcal-actinomyces interactions: H1 utilizes an adhesinlike protein, strain 34 utilizes a polysaccharide structure, and J22 utilizes both of these strategies. This diversity in usage of surface structures may allow these strains to be successful, each within its own econiche.

Evidence for involvement of the H1 polysaccharide in coaggregations to secondary colonizers came later (48). The H1 to *C. ochracea* ATCC 33596 interaction was abolished by heating the capnocytophaga but not the streptococcal partner (48), and the interaction was found to be Rha-inhibitable (49). In another study, the H1 polysaccharide was shown to be accessible for cell-to-cell interactions with a second partner while concurrently interacting with actinomyces in experimental dental plaque formation (50). These results suggest that H1 could be simultaneously bound to actinomyces (via H1 adhesinlike interactions) and to capnocytophaga (with the H1 polysaccharide serving as a bridge) in *in vitro* human dental plaque.

The proposed adhesin binding site on the *S. sanguis* 34 hexasaccharide consists of the two reducing end sugars, GalNAcβ1→3Gal (51). The most effective saccharide inhibitor of the coaggregation between *S. sanguis* H1 and *C. ochreacea* ATCC 33596 is Rha (49, 16). While 2 Rha residues are present within the *S. sanguis* H1 hexasaccharide, the actual site for *C. ochracea* ATCC 33596 adhesin binding is unknown. These studies as well as examinations into the identity of the adhesin on *C. ochracea* ATCC 33596 are ongoing (49; Footnote 2). In addition, the structure of the intact *S. sanguis* H1 polysaccharide is presently being examined. It is apparent through structural studies such as these that the molecular

[2] Weiss, E. I., Eli, I., Smorodinsky, N., and Shenitzky, B. (1989) Abstracts of the Annual Meeting of the American Society for Microbiology, page 115, Washington, D.C.

mechanisms of coaggregation interactions can be determined. Through analysis of polysaccharide structure, analysis of polysaccharide presentation to its partner cells, and through determination of the adhesin binding fine specificity, differences in coaggregation partner specificities can be explained which may allow many complex interactions found in the human oral ecosystem to be better understood.

Acknowledgments—We thank Ramadas Bhat (CCRC, Athens, GA) for conducting the butanolysis and methylation analysis, Edward Sokoloski (NHLBI, Bethesda, MD) for conducting PDMS experiments, and Paul Kolenbrander (NIDR, Bethesda, MD) for helpful suggestions in the preparation of the manuscript.

REFERENCES

1. Weis, W., Brown, J. H., Cusack, S., Paulson, J. C., Skehel, J. J., and Wiley, D. C. (1988) *Nature* **333,** 426–431
2. Markwell, M. A. K. (1986) in *Microbial Lectins and Agglutinins, Properties and Biological Activity* (Mirelman, D., ed) pp. 21–53, John Wiley & Sons, New York
3. Razin, S., and Yogev, D. (1989) in *Molecular Mechanisms of Microbial Adhesion* (Switalski, L., Hoök, M., and Beachey, E., eds) pp. 52–76, Springer-Verlag, New York
4. Razin, S. (1986) in *Microbial Lectins and Agglutinins, Properties and Biological Activity* (Mirelman, D., ed) pp. 217–236, John Wiley & Sons, New York
5. Lev, B., Ward, H., and Pereira, M. E. A. (1986) in *Microbial Lectins and Agglutinins, Properties and Biological Activity* (Mirelman, D., ed) pp. 301–318, John Wiley & Sons, New York
6. Mirelman, D., and Ravdin, J. I. (1986) in *Microbial Lectins and Agglutinins, Properties and Biological Activity* (Mirelman, D., ed) pp. 319–334, John Wiley & Sons, New York
7. Jungery, M., and Weatherall, D. J. (1986) in *Microbial Lectins and Agglutinins, Properties and Biological Activity* (Mirelman, D., ed) pp. 335–358, John Wiley & Sons, New York
8. Mirelman, D. (ed) (1986) *Microbial Lectins and Agglutinins, Properties and Biological Activity*, John Wiley & Sons, New York
9. Sharon, N. (1986) in *The Lectins: Properties, Functions, and Applications in Biology and Medicine* (Liener, I. E., Sharon, N., and Goldstein, I. J., eds) pp. 493–526, Academic Press, Inc., London
10. Karlsson, K.-A. (1989) *Annu. Rev. Biochem.* **58,** 309–350
11. Leffler, H., and Svanborg-Edén, C. (1986) in *Microbial Lectins and Agglutinins, Properties and Biological Activity* (Mirelman, D., ed) pp. 83–112, John Wiley & Sons, New York
12. Parkkinen, J., Rogers, G. N., Korhonen, T., Dahr, W., and Finne, J. (1986) *Infect. Immun.* **54,** 37–42
13. Gibbons, R., and Hay, D. I. (1989) in *Molecular Mechanisms of Microbial Adhesion* (Switalski, L., Hook, M., and Beachey, E., eds) pp. 143–163, Springer-Verlag, New York
14. Roberts, D. D., Olson, L. D., Barile, M. F., Ginsburg, V., and Krivan, H. C. (1989) *J. Biol. Chem.* **264,** 9289–9293
15. McIntire, F. C., Crosby, L. K., Vatter, A. E., Cisar, J. O., McNeil, M. R., Bush, C. A., Tjoa, S. S., and Fennessey, P. V. (1988) *J. Bacteriol.* **170,** 2229–2235
16. Cassels, F. J., and London, J. (1989) *J. Bacteriol.* **171,** 4019–4025
17. Abeygunawardana, C., Bush, C. A., and Cisar, J. O. (1990) *Biochemistry* **29,** 234–248
18. Makela, P. H. (1989) in *Molecular Mechanisms of Microbial Adhesion* (Switalski, L., Hook, M., Beachey, E., eds) pp. 212–221, Springer-Verlag, New York
19. Kolenbrander, P. E. (1988) *Annu. Rev. Microbiol.* **42,** 627–656
20. Kolenbrander, P. E. (1989) *CRC Crit. Rev. Microbiol.* **17,** 137–159
21. Abeygunawardana, C., Bush, C. A., Tjoa, S. S., Fennessey, P. V., and McNeil, M. R. (1989) *Carbohydr. Res.* **191,** 279–293
22. Maryanski, J. H., and Wittenberger, C. L. (1975) *J. Bacteriol.* **124,** 1475–1481
23. Prehm, P., Stirm, S., Jann, B., and Jann, K. (1975) *Eur. J. Biochem.* **56,** 41–55
24. Blumberg, K., Liniere, F., Pustilnik, L., and Bush, C. A. (1982) *Anal. Biochem.* **119,** 407–412
25. Mellis, S. J., and Baenziger, J. U. (1981) *Anal. Biochem.* **114,** 276–280
26. Warren, C. D., Scott, A. S., and Jeanloz, R. W. (1983) *Carbohydr. Res.* **116,** 171–182
27. Lato, M., Brunelli, B., Giuffini, G., and Mezzetti, T. (1968) *J. Chromatogr.* **36,** 191–197
28. York, W. S., Darvill, A. G., McNeil, M., Stevenson, T. T., and Albersheim, P. (1985) *Methods Enzymol.* **118,** 3–40
29. Nagayama, K., Kumar, A., Wüthrich, K., and Ernst, R. R. (1980) *J. Magn. Reson.* **40,** 321–329
30. Bax, A., and Davis, D. G. (1985) *J. Magn. Reson.* **65,** 355–360
31. Marion, D., and Wüthrich, K. (1983) *Biochem. Biophys. Res. Commun.* **113,** 967–974
32. Bax, A. (1982) *Two-dimensional Nuclear Magnetic Resonance in Liquids.* Delft University Press, pp. 51–68, Delft, The Netherlands
33. Bax, A., and Subramanian, S. (1986) *J. Magn. Reson.* **67,** 565–569
34. Shaka, A. J., Barker, P. B., and Freeman, R. (1985) *J. Magn. Reson.* **64,** 547–552
35. Bax A., and Summers, M. F. (1986) *J. Am. Chem. Soc.* **108,** 2093–2094
36. Van Halbeek, H. (1990) in *Frontiers of NMR in Molecular Biology* (Live, D., Armitage, I., and Patel, D., eds) Alan R. Liss, New York, 195–213
37. Powell, D. A. P., York, W. S., Etse, J. T., Gray, A. I., Waterman, P. G., and van Halbeek, H. (1990) *Can. J. Chem.*, in press
38. Massiot, G., Lavaud, C., Le Men-Olivier, L., Van Binst, G., Miller, S. P. F., and Fales, H. M. (1988) *J. Chem. Soc. Perkin Trans.* **1,** 3071–3079
39. Bock, K., and Thøgersen, H. (1982) *Annu. Rep. NMR Spectrosc.* **13,** 1–57
40. Bock, K., Pedersen, C., and Pedersen, H. (1984) *Adv. Carbohydr. Chem. Biochem.* **42,** 193–225
41. Cotter, R. J. (1988) *Anal. Chem.* **60,** 781A–793A
42. Dell, A. (1987) *Adv. Carbohydr. Chem. Biochem.* **45,** 19–72
43. Lerner, L., and Bax, A. (1987) *Carbohydr. Res.* **166,** 35–46
44. Byrd, R. A., Egan, W., Summers, M. F., and Bax, A. (1987) *Carbohydr. Res.* **166,** 47–58
45. Bush, C. A. (1988) *Bull. Magn. Reson.* **10,** 73–95
46. McIntire, F. C., Bush, C. A., Wu, S-S., Li, S-C., Li, Y-T., McNeil, M., Tjoa, S. S., and Fennessey, P. V. (1987) *Carbohydr. Res.* **166,** 133–143
47. Cisar, J. O., Kolenbrander, P. E., and McIntire, F. C. (1979) *Infect. Immun.* **24,** 742–752
48. Kolenbrander, P. E., and Andersen, R. N. (1984) *J. Periodont. Res.* **19,** 564–569
49. Weiss, E. I., London, J., Kolenbrander, P. E., Kagermeier, A. S., and Andersen, R. N. (1987) *Infect. Immun.* **55,** 1198–1202
50. Kolenbrander, P. E., and Andersen, R. N. (1986) *J. Bacteriol.* **168,** 851–859
51. Cisar, J. O., Brennan, M. J., and Sandberg, A. L. (1989) in *Molecular Mechanisms of Microbial Adhesion* (Switalski, L., Hook, M., and Beachey, E., eds) pp. 164–170, Springer-Verlag, New York

QUALITY INSPECTED 1

Accesion For
NTIS CRA&I ☑
DTIC TAB ☐
Unannounced ☐
Justification
By
Distribution /
Availability Codes
Dist | Avail and / or Special
A-1